



# Expression of a Constitutively Active Human Insulin Receptor in Hippocampal Neurons Does Not Alter VGCC Currents

H. N. Frazier<sup>1</sup> · K. L. Anderson<sup>1</sup> · S. Maimaiti<sup>1</sup> · A. O. Ghoweri<sup>1</sup> · S. D. Kraner<sup>3</sup> · G. J. Popa<sup>2</sup> · K. K. Hampton<sup>1</sup> · M. D. Mendenhall<sup>2</sup> · C. M. Norris<sup>3</sup> · R. J. Craven<sup>1</sup> · O. Thibault<sup>1</sup>

Received: 5 December 2017 / Revised: 16 March 2018 / Accepted: 19 March 2018 / Published online: 23 March 2018  
© Springer Science+Business Media, LLC, part of Springer Nature 2018

## Abstract

Memory and cognitive decline are the product of numerous physiological changes within the aging brain. Multiple theories have focused on the oxidative, calcium, cholinergic, vascular, and inflammation hypotheses of brain aging, with recent evidence suggesting that reductions in insulin signaling may also contribute. Specifically, a reduction in insulin receptor density and mRNA levels has been implicated, however, overcoming these changes remains a challenge. While increasing insulin receptor occupation has been successful in offsetting cognitive decline, alternative molecular approaches should be considered as they could bypass the need for brain insulin delivery. Moreover, this approach may be favorable to test the impact of continued insulin receptor signaling on neuronal function. Here we used hippocampal cultures infected with lentivirus with or without IR $\beta$ , a constitutively active, truncated form of the human insulin receptor, to characterize the impact continued insulin receptor signaling on voltage-gated calcium channels. Infected cultures were harvested between DIV 13 and 17 (48 h after infection) for Western blot analysis on pAKT and AKT. These results were complemented with whole-cell patch-clamp recordings of individual pyramidal neurons starting 96 h post-infection. Results indicate that while a significant increase in neuronal pAKT/AKT ratio was seen at the time point tested, effects on voltage-gated calcium channels were not detected. These results suggest that there is a significant difference between constitutively active insulin receptors and the actions of insulin on an intact receptor, highlighting potential alternate mechanisms of neuronal insulin resistance and mode of activation.

**Keywords** Calcium · Electrophysiology · Insulin resistance · Memory

## Abbreviations

IR Insulin receptor  
AHP Afterhyperpolarization  
VGCC Voltage-gated Ca<sup>2+</sup> channel  
SEM Standard error of the mean  
TTX Tetrodotoxin

CICR Calcium-induced calcium-release  
DIV Days in vitro

## Introduction

Insulin signaling in the brain is an integral physiological component of proper neurological function and has been shown to help maintain receptor trafficking (AMPA, NMDA, GABA<sub>A</sub>) [1–5], increase cerebral blood flow [6–10], stimulate glucose transporter translocation [11, 12], reduce voltage-gated calcium channel (VGCC) function [13–15], reduce neuroinflammation [16], and reduce ryanodine receptor function [14]. Studies on age-related alterations in insulin signaling have highlighted a reduction in insulin receptor density and insulin receptor mRNA in aged brains [17–20]. Intranasal insulin administration has been shown to improve cognitive function in both young and aged individuals [21–27] with similar reports in animal models of

✉ O. Thibault  
othibau@uky.edu

<sup>1</sup> Department of Pharmacology and Nutritional Sciences, University of Kentucky Medical Center, UKMC, 800 Rose Street, Lexington, KY 40536, USA

<sup>2</sup> Department of Molecular and Cellular Biochemistry, University of Kentucky Medical Center, UKMC, 741 S. Limestone, Lexington, KY 40536, USA

<sup>3</sup> Sanders Brown Center on Aging, University of Kentucky Medical Center, UKMC, 800 S. Limestone, Lexington, KY 40536, USA

Alzheimer's disease and aging [7, 16, 28–30]. While the mechanism by which insulin exerts these physiological effects is not fully understood, some evidence suggests that it may be related to calcium signaling.

Both classic and contemporary evidence suggests that tight regulation of intracellular calcium levels is required for normal cellular function [31–38]. In response to evidence of neuronal calcium dysregulation in aging, the calcium hypothesis of brain aging was developed [39, 40]. This hypothesis states that calcium dysregulation can lead to cognitive decline by increasing calcium transients, VGCCs, and calcium-mediated afterhyperpolarization (AHP) [41–45]. Our lab has shown that insulin administration leads to a reduction in the slow-AHP in rat hippocampal neurons [7, 29, 46]. Together, this evidence highlights a possible connection between insulin signaling and calcium homeostasis with regards to age-related cognitive decline. These data also suggest that maintaining insulin signaling is a viable therapeutic approach to address this decline [46, 47]. Indeed, others have used administration of a chemical supplement (oxaloacetate) to increase insulin signaling in the brain [48]. Based on these findings, we sought to explore the impact of molecular enhancement of insulin receptor signaling in the absence of exogenous insulin by expressing a truncated, constitutively active human insulin receptor (IR $\beta$ ) in rat primary hippocampal neurons.

IR $\beta$  is a modified human insulin receptor consisting almost solely of the catalytic  $\beta$  subunit of the human insulin receptor [49]. This truncation leads to insertion into the plasma membrane together with constitutive activity of the receptor in mouse fibroblasts. Here we tested the hypothesis that expressing a modified, constitutively active form of the insulin receptor in neurons would increase insulin signaling without the need for exogenous delivery of insulin, and would reduce VGCC currents in hippocampal neurons. We infected mixed primary hippocampal cultures with two lentiviral constructs: synapsin-IR $\beta$ -dTomato and synapsin-IR $\beta$ -mCherry and their respective controls. Each construct consists of a neuronal specific promoter (synapsin) and a fluorescent reporter gene (dTomato or mCherry). Cells were either harvested for protein analysis or recorded using whole-cell patch-clamping methods to quantify VGCC currents 4–7 days following infection. Results show that while constitutive activity was obtained, VGCC current density was unaffected. This result is surprising, given the acute and robust effects of exogenous insulin on VGCC and ryanodine receptor function in hippocampal neurons previously reported by our lab [14]. Ongoing studies are investigating the ability of hippocampal neurons to maintain insulin signaling across time to better define mechanisms of insulin insensitivity in the brain, i.e. down-regulation or desensitization of receptors, together with down-stream signaling pathways.

## Methods

### Cell Culture

Hippocampal mixed (neuron/glia) cultures were prepared as described previously [50–52] and established from E18 Sprague-Dawley rats. E18 fetuses and hippocampi were dissected under a microscope in ice-cold Hank's balanced salt solution (Thermo Fisher Scientific Inc., MA) supplemented with 4.2 mM NaHCO<sub>3</sub> and 12 mM HEPES (pH 7.3). Hippocampi were transferred to 0.25% Trypsin EDTA solution at 37 °C (Thermo Fisher Scientific) and left at room temperature (23 °C) for 11 min. Trypsin was removed and the hippocampi were washed three times with SMEM (Minimum Essential Medium supplemented with 200 mM L-glutamine (Thermo Fisher Scientific) and 35 mM D-glucose). Hippocampi were then titrated and diluted with SMEM to the desired final concentration (100,000 neurons/mL) before being plated in 2 mL aliquots onto 35 mm plastic dishes (Corning Inc., Corning, NY) that were previously coated with 10 mg/mL poly-L-lysine (1 h) for a final cell density of 200,000 cells per dish. Cultured neurons were incubated (37 °C, 5% CO<sub>2</sub>, 95% O<sub>2</sub>) for 24 h before the first medium exchange, when half of the medium was replaced with 90% SMEM and 10% horse serum (Thermo Fisher Scientific). After 3 days in vitro (DIV), half of the media was replaced with SMEM containing horse serum, 5-fluoro-2-doxyuridine, and uridine to stop glial cell growth.

All experiments were conducted following a 24 h exposure to a no serum, low glucose (5.5 mM) MEM to maintain normal glucose oxidation rates and insulin sensitivity [50]. Insulin time-course treatments were performed using 10 nM insulin glulisine diluted in sterile saline (Apidra®, stock solution of 100 U; Sanofi-Aventis, Bridgewater, NJ). As a control for our insulin time course experiments, either a 5 or 30 min saline exposure was used to normalize the data. No significant difference was seen between 5 and 30 min control treatments. All data presented were obtained at room temperature (23 °C).

### Lentiviral Construction and Infection

All hippocampal cultures were infected at a multiplicity of infection (MOI) of 25 (calculated based on cell density). Cells were infected between DIV 6 and 8. Five lentiviral constructs were used as follows: EF1a, EF1a-IR $\beta$ , synapsin-dTomato, synapsin-IR $\beta$ -dTomato, and synapsin-IR $\beta$ -mCherry. The EF1a, EF1a-IR $\beta$ , synapsin-dTomato, and synapsin-IR $\beta$ -dTomato plasmids were constructed by Enzymax LLC. EF1a and EF1a-IR $\beta$  were constructed using an initial pHIV-dTomato vector (gift from Bryan Welm, Addgene plasmid #21374) with an additional EF1a

promoter added via ligation to improve neuronal expression. The human IR $\beta$  protein was ligated into this vector between the XbaI and BamHI sites via PCR and standard digestion protocols. Synapsin-dTomato and synapsin-IR $\beta$ -dTomato were also constructed from pHIV-dTomato. The neuronal-specific synapsin promoter was ligated between the AgeI and EcoRI sites and the human IR $\beta$  protein was ligated between the XbaI and BamHI sites using PCR and standard digestion protocols. The synapsin-IR $\beta$ -mCherry plasmid was constructed using an pHR-SFFV-KRAB-dCas9-P2A-mCherry vector (gift of Jonathan Weissman, Addgene plasmid #60954). The self-cleaving P2A site preceding the mCherry sequence produces mCherry expression at a 1:1 ratio with the IR $\beta$  protein, thus improving fluorescence. The synapsin promoter and human IR $\beta$  protein were ligated into the vector between the AscI and BamHI sites, replacing the Cas9 sequence via PCR and standard digestion protocols. All segments constructed using PCR were sequenced to verify fidelity. All plasmids were then converted into lentiviruses by co-transfecting HEK293 cells with the donor plasmid, PsPAX2, and pMD2.G (gifts from Dr. Didier Trono, Addgene plasmids #12260 and #12259) using a polyethyleneimine (80  $\mu$ g/mL, nominal MW 40,000, pH 7) and NaCl (75 mM) mixture to induce uptake of the DNA. Culture supernatants were withdrawn over a 5-day period, clarified by centrifugation, and the virus precipitated with polyethylene glycol (1.4% w/v) and NaCl (50 mM). The viral pellet was resuspended in cold PBS. Lentiviruses were stored at  $-80^{\circ}\text{C}$  until needed. Viruses were then thawed on ice and immediately administered to culture dishes. mCherry expression was monitored using a Nuance spectral analysis camera (CRi, Inc., Boston, MA). Phase and fluorescence photomicrographs were overlaid in Adobe Photoshop.

### Protein Harvest and Western Blots

Mixed primary hippocampal cells were harvested in RIPA buffer containing phosphatase and protease inhibitors. Cells were further lysed using polytron agitation. Protein levels were quantified using a BCA assay and a microplate reader. Western blots were used to quantify differences in protein expression. Samples were run in duplicate within and across gels and were averaged. Proteins were assessed with the following antibodies: AKT #4685S 1:1000 and pAKT #4051S 1:1000 (Cell Signaling Technology, Inc., Danvers, MA). Blots were developed with chemiluminescence and digitally imaged on a scanner (G-Box; Syngene, Frederick, MD). Gray values were obtained using the ImageJ gel analysis tool (Version 1.46r; Wayne Rasband, National Institute of Health, Rockville, MD). For each blot, mean gray value of pAKT and AKT were normalized to a saline-treated sample, and pAKT was divided by AKT to generate ratios.

### Immunocytochemistry

Primary hippocampal cultures, uninfected or infected with syn-IR $\beta$ -dTomato lentivirus, were fixed using 4% paraformaldehyde (PFA) in 1X PBS for 20 min. Immunocytochemistry was performed using a primary antibody targeted to the HA-tag present on our truncated IR $\beta$  protein (HA-Tag #3724S 1:1600, Cell Signaling Technology) in conjunction with a fluorescent secondary antibody (Alexa Fluor® 488 #A-11070 1:200, Thermo Fisher Scientific). Cultures were imaged using a spectral camera (Nuance FX, CRi, Inc.) and a FITC dichroic mirror equipped with a long-pass emission filter ( $>525$  nm). A series of images were acquired from 490 to 650 nm and were used to define the green and all other fluorescent signals (autofluorescence and background). The green channel was extracted from the total fluorescent signal using the Nuance algorithm (spectral library subtraction).

### VGCC Recording Solutions

For whole-cell recordings of VGCC currents, the external solution was prepared as follows (in mM): 111 NaCl, 5 BaCl $\cdot$ H $_2$ O, 5 CsCl, 2 MgCl $_2$ , 10 g glucose, 10 HEPES, 20 TEACl $\cdot$ H $_2$ O. The solution was brought to pH 7.35 with NaOH and 500 nM tetrodotoxin (TTX) was added before recording to inhibit Na $^+$  channels. The internal pipette solution was prepared as follows (in mM): 145 MsOH, 10 HEPES, 3 MgCl $_2$ , 11 EGTA, 1 CaCl $_2$ , 13 TEACl $\cdot$ H $_2$ O, 14 phosphocreatine Tris-salt, 4 Tris-ATP, 0.3 Tris-GTP. The solution was brought to pH 7.3 with CsOH. All solutions were sterile filtered using a 0.22  $\mu$ m vacuum filter (Corning).

### Whole-Cell Recording and Analysis

All electrophysiological data were acquired between DIV 13 and 17, 4–7 days post-infection. 1.5 mm glass whole-cell patch-clamp electrodes (Drummond Scientific, Broomall, PA) were made using a P-87 micropipette puller (Sutter Instruments, Novato, CA). The culture dish was rinsed with recording solution three times, then filled with 3 mL of the extracellular solution supplemented with 500 nM TTX. To allow for currents to stabilize, all data were recorded 3 min after the whole-cell configuration was achieved. *IV* (current–voltage) relationships ( $-60$  to  $+30$  mV) were initially conducted to identify maximal current voltage. In Figs. 2 and 3, an increase in current density is seen between the *IV* data and the current density data presented in bar graph form. This is likely because *IV*s were conducted 3–5 min prior to peak VGCC current measures. Cells were held at  $-70$  mV and currents were elicited (150 ms) at the maximal peak response derived from the *IV*. All currents were leak subtracted using 5–8 scaled hyperpolarizing sub-pulses. Because insulin may alter cell size, we report on measures

of current densities (pA/pF) derived from dividing maximal current amplitude (average of 5 depolarizations taken 30 s apart) by membrane capacitance (measured in pCLAMP™) for each cell. All electrophysiological data were collected between 4 and 7 days post-lentiviral infection. All recordings were conducted on the stage of an E600FN microscope (Nikon Inc., Melville, NY) placed on an anti-vibration table. An Axopatch 1D (Molecular Devices, Sunnyvale, CA) in combination with a digidata 1200 AD board and pCLAMP™ 7 (Molecular Devices) were used for electrophysiology acquisition. Data were digitized at 5–10 KHz, low-pass filtered at 2–5 KHz, and were quantified in Clampfit 7 (Molecular Devices).

### Statistical Analysis

Electrophysiological results are based on a total of 76 hippocampal neurons obtained from the pups of 6 pregnant dams. Statistical outliers (> 2 standard deviations from the mean) in each data set were excluded from further analysis. Transgene effects on endpoint measures were determined with unpaired t-tests and ANOVAs, and Bonferroni post hoc tests, when necessary. Significance for all comparisons was set at  $p < 0.05$ .

## Results

### Western Blot Analyses

We used Western blot techniques to quantify the ratio of pAKT/AKT in mixed hippocampal cultures treated 5–30 min with 10 nM insulin (Fig. 1a). By 15 min of activation a trend for an increase in signaling was noted ( $n = 3$ ; one-way ANOVA  $p = 0.06$ ), and by 30 min, the pAKT/AKT signal was significantly elevated compared to 30-min saline controls ( $n = 3$ ;  $p < 0.05$ ). Elevated levels of pAKT/AKT at 15 and 30 min confirm continued IR activity at these time points and suggest signaling in neurons increases with ligand exposure time.

To test for constitutive activity of the truncated, human IR $\beta$  receptor in the absence of exogenous insulin, we infected hippocampal cultures (DIV 6–8) with EF1a or EF1a-IR $\beta$  lentiviruses. Cells were harvested for Western blot 48 h post-infection to allow adequate time for protein expression. Cells expressing IR $\beta$  showed significantly elevated pAKT/AKT compared to cells infected with the EF1a negative control (Fig. 1c, d,  $n = 3$ ; t-test  $p < 0.005$ ). Compared to the ligand-derived 30-min time point (Fig. 1a), the increase in signaling was smaller, nearly reaching a threefold increase at 48 h. Thus, compared to control conditions, the IR $\beta$  receptor was expressed and yielded an increase in activity. The results

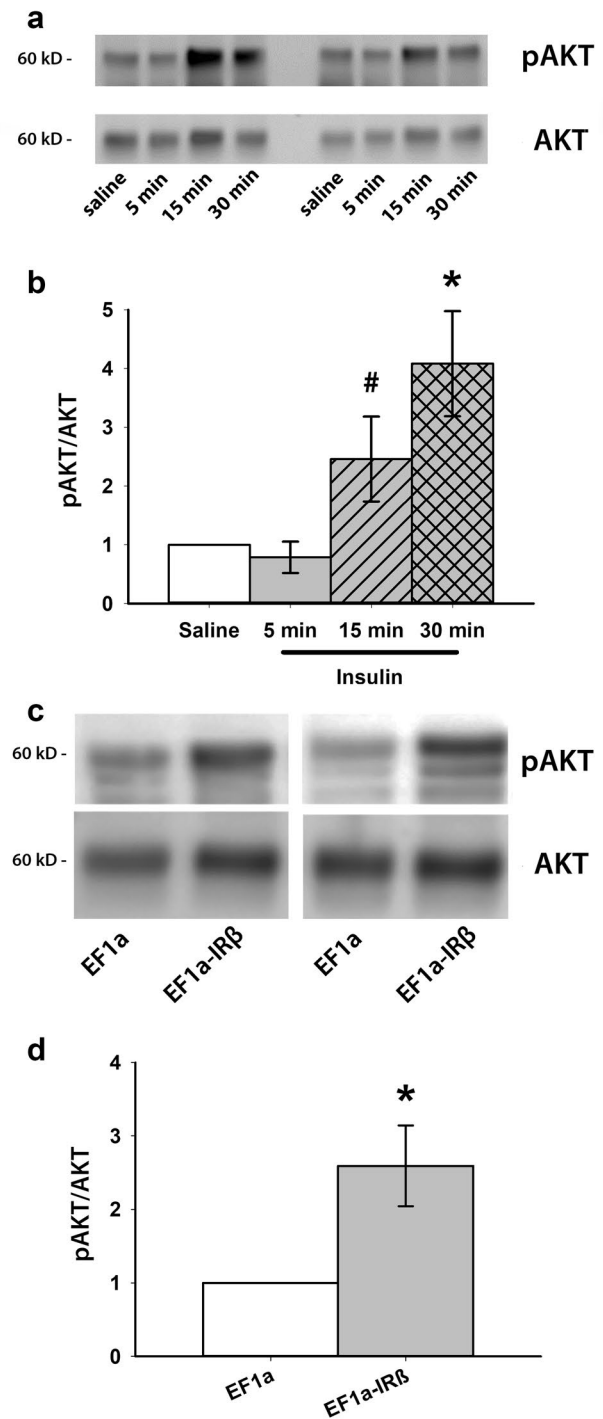


**Fig. 1** Insulin signaling with and without exogenous insulin. **a** Representative Western blots of mixed primary hippocampal cultures treated with saline or 10 nM Apidra® for 5, 15, or 30 min. Each sample was run in duplicate and probed separately across gels. Blots were probed with Cell Signaling Technology anti-phospho AKT (Ser473; #4051) 1:1000 and total AKT (pan #4685) 1:1000. **b** Quantification reveals signaling increases after 15 (trend #) and 30 min compared to timed saline controls ( $n = 3$ ). **c** Representative Western blots of mixed primary hippocampal cultures infected with Ef1a or EF1a-IR $\beta$  lentiviruses. Each sample was run in duplicate and probed separately across gels. Blots were probed as in **b**. **d** Western blot quantification reports significant pAKT/AKT between EF1a and EF1a-IR $\beta$ , suggesting constitutive activity ( $n = 3$ ). # indicates  $p < 0.10$ ; \* indicates  $p < 0.05$ . All data represent means  $\pm$  SEM

also confirm that the infection protocol resulted in constitutive activity in the absence of added insulin.

### Electrophysiological Analyses of the IR $\beta$ Construct Containing IRES and dTomato

To test whether elevated insulin signaling altered VGCC currents, we performed whole-cell patch-clamp experiments on hippocampal neurons infected with either the negative control (syn-dTomato) or IR $\beta$ -containing lentiviruses (syn-IR $\beta$ -dTomato) (Fig. 2a). Cultures were placed in a low glucose, no serum growth media for 24 h prior to electrophysiology recordings on days 4–7 post-infection. A subset of cultures infected with syn-IR $\beta$ -dTomato were fixed for immunocytochemistry staining in order to confirm IR $\beta$  expression using the HA reporter tag present on the IR $\beta$  protein. Anti-HA fluorescent antibody indicated successful expression of IR $\beta$  in approximately 80% of neurons (Fig. 2b, bottom). Live pyramidal neurons were patched and passive membrane properties were recorded from a holding potential of  $-70$  mV. Neither cell capacitance, holding current at  $-70$  mV, nor membrane resistance were found to be different (Table 1). For each cell recorded, we then determined the voltage necessary to elicit maximal current amplitude using an *IV* protocol ( $-60$  to  $+30$  mV). *IV* recordings (Fig. 2c, d) from negative control and IR $\beta$ -expressing neurons were averaged and compared between groups ( $n=30$  per group). No significant difference in VGCC current threshold or peak voltages were seen between groups (Fig. 2d; one-way ANOVA with Bonferroni post hoc  $p>0.05$ ).

For each neuron, VGCC activity generated during the maximum activation voltage step was measured at three different time points: i.e. at peak activity (peak), during the last 10 ms of the voltage step (late), and 50 ms after the voltage step (tail) (Fig. 2e). Current activity at each time point was statistically comparable in neurons expressing IR $\beta$  or d-Tomato control ( $n=30$  per group; two-way ANOVA with Bonferroni post hoc  $p>0.05$ ). This indicates that neither maximal flux through VGCCs, nor the number of available channels, nor the inactivation or deactivation rates were affected by constitutive insulin signaling. Note that current recordings were performed 3–5 min after recording of the *IV* to allow the cell to stabilize. This is likely the reason for the small increase in currents reported between *IV*s (Fig. 2d) and maximal currents (Fig. 2e). To isolate L-type VGCC currents from currents arising from other VGCC subtypes, cells were held at  $-40$  mV for 3 min to inactivate N- and T-type channels. The membrane voltage was then stepped to the voltage necessary to elicit maximal current amplitude. Under these conditions, the presence of IR $\beta$  still had no statistically significant effects on peak, late, or tail current activity (data not shown).

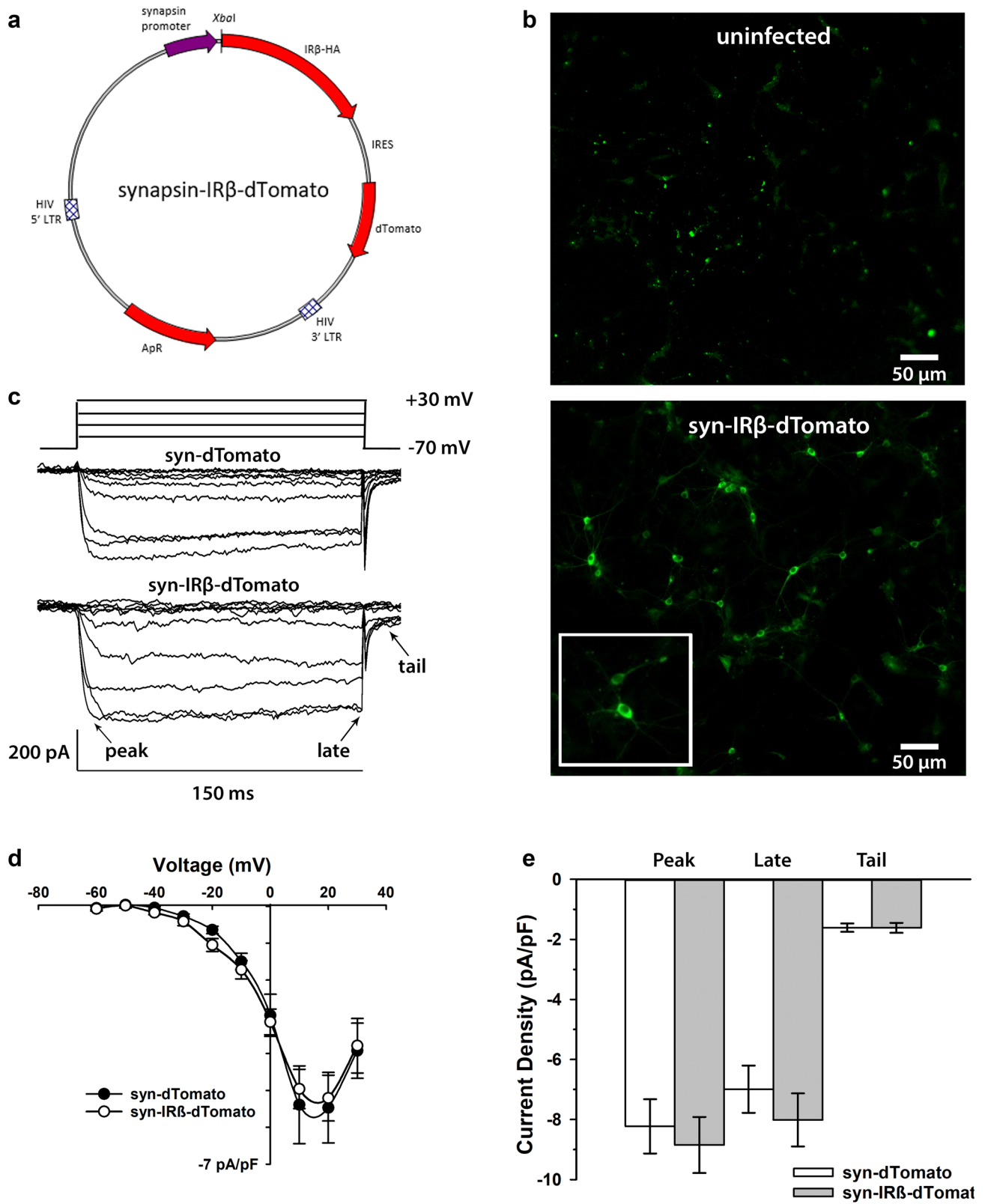
### Electrophysiological Analyses of the IR $\beta$ Construct Containing P2A and mCherry

Because the IRES sequence does not always drive equal expression of the constitutive active IR $\beta$  subunit with the reporter gene (dTomato) [53, 54], we constructed another plasmid using a P2A site and mCherry as the reporter gene (Fig. 3a). This approach yielded more reliable expression of the red fluorescent protein and allowed us to test a second IR $\beta$ -expressing plasmid, therefore providing a more thorough characterization of the impact of sustained insulin signaling on VGCCs. For this series of experiments and because mCherry conferred a higher level of fluorescence compared to dTomato we compared IR $\beta$ -expressing neurons (red) to uninfected (dark) neurons in the same field-of-view (Fig. 3b).

Pyramidal neurons were patched and peak currents were derived following the same *IV* protocol previously described (Fig. 3c). *IV* recordings from control (uninfected) and IR $\beta$ -expressing (syn-IR $\beta$ -mCherry) neurons were averaged and compared. No significant difference in *IV* trace recordings was seen between these two groups of cells (Fig. 3d,  $n=9$  per group; one-way ANOVA with Bonferroni post hoc  $p>0.05$ ). Analysis of maximal currents at peak, late, and tail were then averaged for each cell type. Current recordings from primary hippocampal neurons expressing IR $\beta$  did not show a significant difference compared to uninfected controls at any time point ( $n=9$  per group; two-way ANOVA with Bonferroni post hoc  $p>0.05$ ). As in Fig. 2, VGCCs recorded from a holding potential of  $-40$  mV to increase participation of L-type VGCC, also were not changed by treatment and no significant differences were detected between uninfected and IR $\beta$ -expressing neurons at any time point (data not shown).

### Discussion

The original intent of this study was to circumvent the need for the ligand at the insulin receptor by expressing a constitutively active form of the human insulin receptor in hippocampal neurons. The lack of protein quantification from cells infected with either synapsin-containing vectors (Figs. 2, 3) prevents us from comparing VGCC effect size between these two conditions (synapsin-IR $\beta$ -dTomato versus synapsin-IR $\beta$ -mCherry). This is not a major concern given the lack of an overall effect on VGCC. Further, because IRES-dependent expression of the downstream gene (reporter gene) can be significantly lower than the protein of interest [53, 54], we switched to a P2A-dependent vector to confer comparable levels of expression of both gene products. Even with strong mCherry expression (Fig. 3b), red cells showed no significant differences when compared



to dark cells on measures of VGCC properties. Nevertheless, we show here that viral delivery of a truncated, human insulin receptor ( $IR\beta$ ) increased signaling through pAKT/

AKT in hippocampal neurons. Interpretation of these data highlights potential interplays between insulin signaling and calcium homeostasis in neurons, and may also provide clues

**Fig. 2** Constitutive activity of the human truncated insulin receptor  $\beta$  subunit does not alter voltage sensitivity of VGCCs. **a** Plasmid map of synapsin-dTomato construct. The IR $\beta$  sequence was inserted between XbaI and BamHI sites using PCR ligation for production of the synapsin-IR $\beta$ -dTomato plasmid. **b** Photomicrograph of hippocampal neurons probed for IR $\beta$  expression using a fluorescent HA-tag antibody. Cells in green indicate presence of IR $\beta$ . **c** Representative inward currents obtained from a holding potential of  $-70$  mV during determination of *IV* relationships ( $-60$  to  $+30$  mV). **d** Quantification of VGCC currents across groups and voltages showed no significant difference. **e** Current density (pA/pF) of peak, late, and 50 ms tail currents were not altered by production of the constitutively active form of the human brain insulin receptor. All data represent means  $\pm$  SEM

about intracellular markers used as reporters of insulin sensitivity in neurons.

### Why Study Long-Term Insulin Receptor Activation in Neurons?

We and others have shown that acute applications of insulin can reduce VGCC function [13–15] as well as ryanodine receptor function within minutes [14]. Given that VGCCs and calcium-induced calcium release (CICR) participate in the generation of the AHP [55–59], and that larger calcium-dependent AHPs are seen in neurons from aged, cognitively impaired animals [44, 60, 61], our initial work used repeated daily applications of intranasal insulin to restore calcium homeostasis and redress cognitive decline in aged animals [7, 29]. However, because neuronal IR signaling can last for extended periods of time, we used electrophysiological techniques to characterize VGCC function in hippocampal neurons following 3–7 days of constitutive insulin receptor activity. We sought to identify a novel therapeutic approach to maintain calcium homeostasis by providing constitutive insulin signaling.

Results indicate that expressing three different IR $\beta$ -containing plasmid constructs and their controls in neurons raised downstream signaling from the insulin receptor for at least 72 h, yet VGCC currents were not affected, even 7 days post-infection. This result is surprising given our previous work showing that acute insulin administration in

hippocampal neurons can reduce calcium-sensitive functions. Potential explanations for these results include, but are not limited to, the impact of insulin signaling duration and the activation of different downstream signaling pathways.

### Is Time Important?

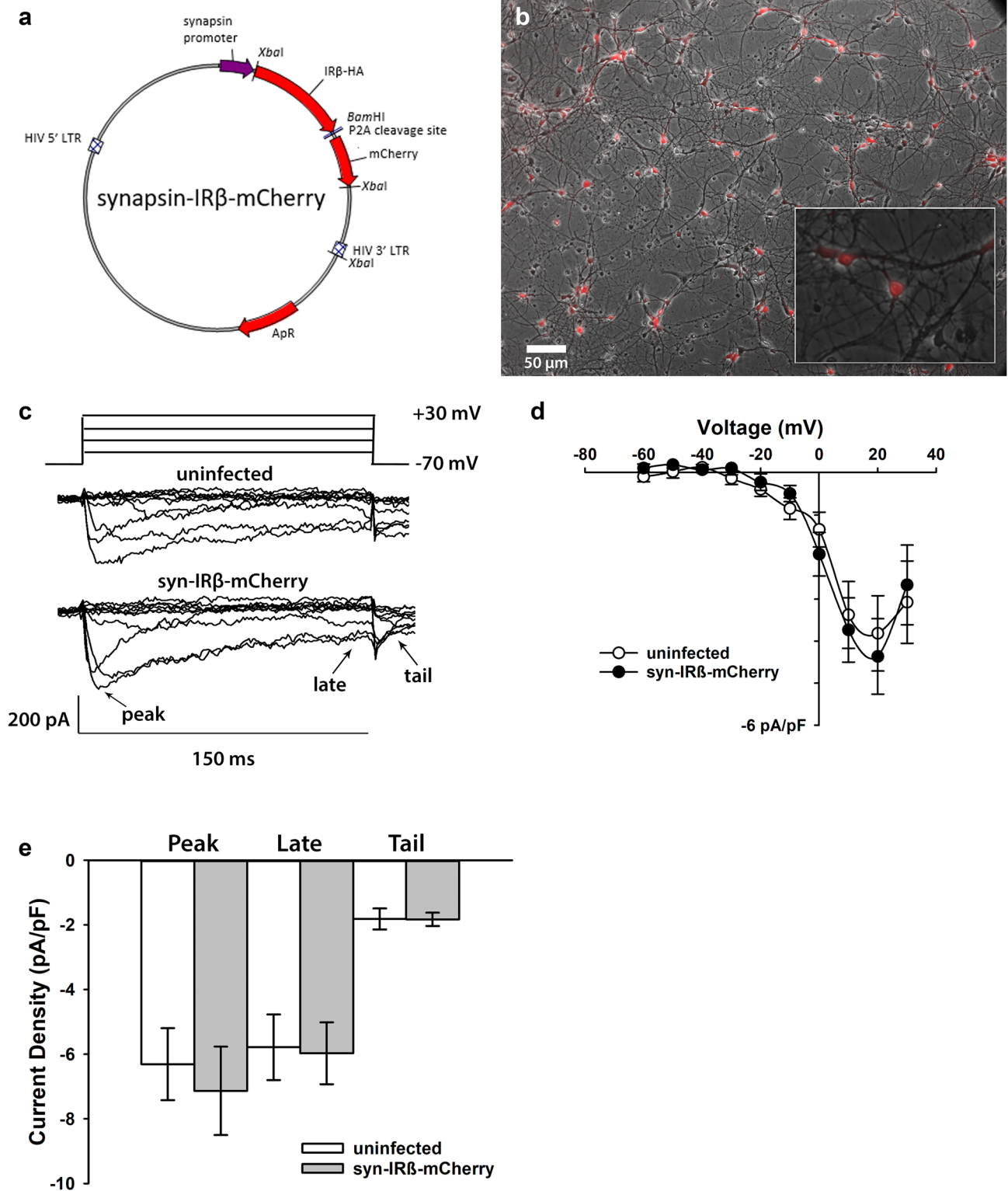
In contrast to insulin signaling in the periphery where activation is quickly terminated by internalization of the IR in muscle and fat cells [62–65], neuronal IRs can signal for long periods of time without evidence of down-regulation [49, 66]. While we present evidence of long-term (72 h) insulin receptor signaling via IRS/PIP<sub>3</sub>/AKT, these results suggest that continued activation of this pathway does not reduce VGCCs in neurons. Further, we recently showed that reductions in neuronal calcium levels and calcium-mediated potentials were not seen in the ZDF rat even following a 7-week period of sustained peripheral hyperglycemia and hyperinsulinemia [29]. Additionally, activation of the PI3K/mTOR/AKT pathway was shown to rapidly increase synaptic protein levels within minutes [67], while other pathways, such as MEK/ERK, a pathway which has nuclear targets, have been implicated in modulating the expression of calcium-sensitive channels [68]. It follows that targeting nuclear factors would be slower and likely longer-lasting compared to pathways involved with acute IR activation. Based on the evidence presented here, we propose that signaling pathways other than AKT must exist in neurons to alter long-term calcium homeostasis.

An alternative interpretation is that the molecular approach was successful at reducing VGCCs but only transiently, and at an earlier time than tested here. Unfortunately, the acute impact of lentiviral delivery on VGCCs cannot be determined because of the time constraints associated with changes in protein expression. Standard lentiviral protocols require an incubation period of at least 24–48 h before adequate expression of the protein is reached. Thus, these experimental protocols did not allow us to test for VGCC changes within the same time frame as acute insulin exposures (i.e. 10 min). Given the long-lasting nature of insulin

**Table 1** Cellular and electrode parameters

	Synapsin-dTomato	Synapsin-IR $\beta$ -dTomato	Uninfected	Synapsin-IR $\beta$ -mCherry
Membrane capacitance (pF)	71.90 $\pm$ 3.60	66.10 $\pm$ 3.53	59.36 $\pm$ 3.95	67.46 $\pm$ 5.78
Membrane resistance (M $\Omega$ )	450.30 $\pm$ 45.34	555.20 $\pm$ 42.48	528.90 $\pm$ 95.84	322.79 $\pm$ 39.11
Access resistance (M $\Omega$ )	11.60 $\pm$ 0.86	11.10 $\pm$ 0.69	9.87 $\pm$ 1.20	9.13 $\pm$ 0.50
Holding current (pA)	$-131.00 \pm 14.35$	$-98.29 \pm 13.56$	$-86.77 \pm 12.08$	$-147.94 \pm 22.93$

Data represents means  $\pm$  SEM obtained from four different groups of cells (n=78) studied under patch-clamping conditions to record VGCC currents. No significant difference was detected between the groups



signaling in neurons, it is clear that future studies are needed to investigate the impact of time on several IR pathways.

### What is Neuronal Insulin Resistance?

Evidence for insulin resistance in neurons has been derived from a multitude of molecular experiments showing reductions in signaling from the level of the insulin receptor and

**Fig. 3** A second constitutively active form of the human truncated insulin receptor  $\beta$  subunit does not alter voltage sensitivity of VGCCs. **a** Plasmid map of synapsin-mCherry IR $\beta$  subunit construct. Note replacement of the IRES sequence with the P2A site. The IR $\beta$  sequence was inserted between XbaI and BamHI sites using PCR ligation for production of the synapsin-IR $\beta$ -mCherry plasmid. **b** Photomicrograph of cultured neurons exposed 48 h to the synapsin-IR $\beta$ -mCherry, we estimate ~70–80% infection efficacy. Uninfected cells (dark) were used as controls. Inset shows both fluorescent and non-fluorescent cells. **c** Representative inward currents obtained from a holding potential of  $-70$  mV during determination of *IV* relationships ( $-60$  to  $+30$  mV). **d** Quantification of VGCC currents across groups shows no significant difference. **e** Current density (pA/pF) of peak, late, and 50 ms tail were not altered by production of this second constitutively active form of the human insulin receptor. All data represent means  $\pm$  SEM

IRS1 to GLUT4 [69–74]. While inhibition at any point in this cascade negatively impacts insulin signaling, it is not clear which single point best reflects the phenomenon described as insulin resistance; despite this, focus has historically been placed on AKT. Our evidence of maintained pAKT signaling in the absence of detectable changes in VGCC suggests that observation of AKT phosphorylation by itself may not be a representative indicator of insulin sensitivity in neurons. Additionally, because multiple proteins within the insulin signaling pathway are also sensitive to other agents and cross signaling, analysis of one single aspect of the IR signaling cascade does not specifically assess insulin resistance in the tissue. Therefore, alternative methods for quantifications of insulin sensitivity perhaps need to be considered.

We have used insulin administration to directly test insulin sensitivity in hippocampal neurons in slices of young and aged animals. In these studies, the impact of exogenous insulin has repeatedly been greater in aged compared to young neurons [29, 46]. Further, using magnetic resonance spectroscopy (MRS) and cerebral blood-flow data, we also show a greater impact of insulin in aged compared to young brains [7]. Acute application of the anti-diabetic drug pioglitazone on hippocampal slices also provides evidence for greater sensitivity of the drug in aged animals compared to young [75]. Evidence from other groups shows reductions in blood–brain barrier insulin transport may be responsible for the aged-dependent reduction in insulin sensitivity [76]. In this paper, the author presents evidence that phosphorylation of AKT in aged mice treated with intracerebroventricular injections of insulin is comparable to that seen in young mice. Finally, in animal models of Alzheimer’s disease, a greater increase in hippocampal insulin receptor signaling was seen in mid-age compared to young mice [77]. Together, these data suggest that the underlying insulin sensitivity and in particular, the definition of this sensitivity in neurons needs further clarification.

## Future Directions and Conclusions

It is clear a more detailed characterization of insulin resistance in neurons is needed in order to better define new and targetable therapies. With respect to the potential impact of insulin and its neuroprotective role in neurons (i.e. reducing calcium influx), much remains unknown, and it is unclear whether the short-acting PI3K pathway or the likely longer pathway through ERK is involved. Also, attention to the sub-cellular compartmentalization of the modified insulin pathway with aging and Alzheimer’s disease is needed. This is likely important, given the evidence that insulin receptors concentrate at synaptic sites [78–80], and a greater focus on post-synaptic densities, where crucial insulin-sensitive ion targets are located should be considered [81].

Overall, it appears we have identified a neuronal model of insulin resistance in the presence of increased pAKT activation. While neuronal insulin insensitivity has been proposed as a contributor to age-related cognitive decline, the mechanisms behind this are not well understood. Specifically, further studies are needed to characterize downstream cellular targets of neuronal insulin receptor activation (e.g., glucose utilization, glucose transporters, calcium transporters, calcium buffers, ER calcium homeostasis and others), and to provide a fuller picture of neuronal insulin resistance with age. Greater definition of insulin receptor desensitization, internalization and the mechanisms involved in down-regulation of IR signaling in neurons need investigation in animal models of aging.

**Acknowledgements** We acknowledge the National Institute of Health for sources of funding for these experiments: Thibault, O. (R01AG033649); Frazier, H. and Hampton, K.K. (T32DK007778). The authors acknowledge the use of facilities in the University of Kentucky Center for Molecular Medicine Genetic Technologies Core. This core is supported in part by National Institute of Health Grant Number P30GM110787.

## References

1. Lin JW, Ju W, Foster K, Lee SH, Ahmadian G, Wyszynski M, Wang YT, Sheng M (2000) Distinct molecular mechanisms and divergent endocytotic pathways of AMPA receptor internalization. *Nat Neurosci* 3(12):1282–1290. <https://doi.org/10.1038/81814>
2. Man HY, Lin JW, Ju WH, Ahmadian G, Liu L, Becker LE, Sheng M, Wang YT (2000) Regulation of AMPA receptor-mediated synaptic transmission by clathrin-dependent receptor internalization. *Neuron* 25(3):649–662
3. Skeberdis VA, Lan J, Opitz T, Zheng X, Bennett MV, Zukin RS (2001) mGluR1-mediated potentiation of NMDA receptors involves a rise in intracellular calcium and activation of protein kinase C. *Neuropharmacology* 40(7):856–865
4. Vetiska SM, Ahmadian G, Ju W, Liu L, Wymann MP, Wang YT (2007) GABAA receptor-associated phosphoinositide 3-kinase is required for insulin-induced recruitment of postsynaptic GABAA

- receptors. *Neuropharmacology* 52(1):146–155. <https://doi.org/10.1016/j.neuropharm.2006.06.023>
5. Wan Q, Xiong ZG, Man HY, Ackerley CA, Braunton J, Lu WY, Becker LE, MacDonald JF, Wang YT (1997) Recruitment of functional GABA(A) receptors to postsynaptic domains by insulin. *Nature* 388(6643):686–690. <https://doi.org/10.1038/41792>
  6. Akintola AA, van Opstal AM, Westendorp RG, Postmus I, van der Grond J, van Heemst D (2017) Effect of intranasally administered insulin on cerebral blood flow and perfusion: a randomized experiment in young and older adults. *Aging (Albany NY)* 9(3):790–802. <https://doi.org/10.18632/aging.101192>
  7. Anderson KL, Frazier HN, Maimaiti S, Bakshi VV, Majeed ZR, Brewer LD, Porter NM, Lin AL, Thibault O (2016) Impact of single or repeated dose intranasal zinc-free insulin in young and aged F344 rats on cognition, signaling, and brain metabolism. *J Gerontol A*. <https://doi.org/10.1093/gerona/glw065>
  8. Novak V, Milberg W, Hao Y, Munshi M, Novak P, Galica A, Manor B, Roberson P, Craft S, Abduljalil A (2014) Enhancement of vasoreactivity and cognition by intranasal insulin in type 2 diabetes. *Diabetes Care* 37(3):751–759. <https://doi.org/10.2337/dc13-1672>
  9. Rajasekar N, Nath C, Hanif K, Shukla R (2017) Intranasal insulin improves cerebral blood flow, Nrf-2 expression and BDNF in STZ (ICV)-induced memory impaired rats. *Life Sci* 173:1–10. <https://doi.org/10.1016/j.lfs.2016.09.020>
  10. Schilling TM, Ferreira de Sa DS, Westerhausen R, Strelzyk F, Larra MF, Hallschmid M, Savaskan E, Oitzl MS, Busch HP, Naumann E, Schachinger H (2014) Intranasal insulin increases regional cerebral blood flow in the insular cortex in men independently of cortisol manipulation. *Hum Brain Mapp* 35(5):1944–1956. <https://doi.org/10.1002/hbm.22304>
  11. Grillo CA, Piroli GG, Hendry RM, Reagan LP (2009) Insulin-stimulated translocation of GLUT4 to the plasma membrane in rat hippocampus is PI3-kinase dependent. *Brain Res* 1296:35–45. <https://doi.org/10.1016/j.brainres.2009.08.005>
  12. McNay EC, Sandusky LA, Pearson-Leary J (2013) Hippocampal insulin microinjection and in vivo microdialysis during spatial memory testing. *J Vis Exp (71):e4451*. <https://doi.org/10.3791/4451>
  13. Chik CL, Li B, Karpinski E, Ho AK (1997) Insulin and insulin-like growth factor-I inhibit the L-type calcium channel current in rat pinealocytes. *Endocrinology* 138(5):2033–2042. <https://doi.org/10.1210/endo.138.5.5129>
  14. Maimaiti S, Frazier HN, Anderson KL, Ghoweri AO, Brewer LD, Porter NM, Thibault O (2017) Novel calcium-related targets of insulin in hippocampal neurons. *Neuroscience* 364:130–142. <https://doi.org/10.1016/j.neuroscience.2017.09.019>
  15. Stella SL Jr, Bryson EJ, Thoreson WB (2001) Insulin inhibits voltage-dependent calcium influx into rod photoreceptors. *Neuroreport* 12(5):947–951
  16. Adzovic L, Lynn AE, D'Angelo HM, Crockett AM, Kaercher RM, Royer SE, Hopp SC, Wenk GL (2015) Insulin improves memory and reduces chronic neuroinflammation in the hippocampus of young but not aged brains. *J Neuroinflamm* 12:63. <https://doi.org/10.1186/s12974-015-0282-z>
  17. Frolich L, Blum-Degen D, Bernstein HG, Engelsberger S, Humrich J, Laufer S, Muschner D, Thalheimer A, Turk A, Hoyer S, Zochling R, Boissl KW, Jellinger K, Riederer P (1998) Brain insulin and insulin receptors in aging and sporadic Alzheimer's disease. *J Neural Transm (Vienna)* 105(4–5):423–438. <https://doi.org/10.1007/s007020050068>
  18. Zaia A, Piantanelli L (1996) Alterations of brain insulin receptor characteristics in aging mice. *Arch Gerontol Geriatr* 23(1):27–37
  19. Zhao WQ, Chen H, Quon MJ, Alkon DL (2004) Insulin and the insulin receptor in experimental models of learning and memory. *Eur J Pharmacol* 490(1–3):71–81. <https://doi.org/10.1016/j.ejphar.2004.02.045>
  20. Stranahan AM (2015) Models and mechanisms for hippocampal dysfunction in obesity and diabetes. *Neuroscience* 309:125–139. <https://doi.org/10.1016/j.neuroscience.2015.04.045>
  21. Benedict C, Hallschmid M, Hatke A, Schultes B, Fehm HL, Born J, Kern W (2004) Intranasal insulin improves memory in humans. *Psychoneuroendocrinology* 29(10):1326–1334. <https://doi.org/10.1016/j.psyneuen.2004.04.003>
  22. Brunner YF, Kofeet A, Benedict C, Freiherr J (2015) Central insulin administration improves odor-cued reactivation of spatial memory in young men. *J Clin Endocrinol Metab* 100(1):212–219. <https://doi.org/10.1210/jc.2014-3018>
  23. Craft S, Baker LD, Montine TJ, Minoshima S, Watson GS, Claxton A, Arbuckle M, Callaghan M, Tsai E, Plymate SR, Green PS, Leverenz J, Cross D, Gerton B (2012) Intranasal insulin therapy for Alzheimer disease and amnesic mild cognitive impairment: a pilot clinical trial. *Arch Neurol* 69(1):29–38. <https://doi.org/10.1001/archneurol.2011.233>
  24. de la Monte SM (2012) Early intranasal insulin therapy halts progression of neurodegeneration: progress in Alzheimer's disease therapeutics. *Aging Health* 8(1):61–64. <https://doi.org/10.2217/ahe.11.89>
  25. Freiherr J, Hallschmid M, Frey WH 2nd, Brunner YF, Chapman CD, Holscher C, Craft S, De Felice FG, Benedict C (2013) Intranasal insulin as a treatment for Alzheimer's disease: a review of basic research and clinical evidence. *CNS Drugs* 27(7):505–514. <https://doi.org/10.1007/s40263-013-0076-8>
  26. Reger MA, Watson GS, Frey WH 2nd, Baker LD, Cholerton B, Keeling ML, Belongia DA, Fishel MA, Plymate SR, Schellenberg GD, Cherrier MM, Craft S (2006) Effects of intranasal insulin on cognition in memory-impaired older adults: modulation by APOE genotype. *Neurobiol Aging* 27(3):451–458. <https://doi.org/10.1016/j.neurobiolaging.2005.03.016>
  27. Reger MA, Watson GS, Green PS, Baker LD, Cholerton B, Fishel MA, Plymate SR, Cherrier MM, Schellenberg GD, Frey WH 2nd, Craft S (2008) Intranasal insulin administration dose-dependently modulates verbal memory and plasma amyloid-beta in memory-impaired older adults. *J Alzheimers Dis* 13(3):323–331
  28. Apostolatos A, Song S, Acosta S, Peart M, Watson JE, Bickford P, Cooper DR, Patel NA (2012) Insulin promotes neuronal survival via the alternatively spliced protein kinase CdeltaII isoform. *J Biol Chem* 287(12):9299–9310. <https://doi.org/10.1074/jbc.M111.313080>
  29. Maimaiti S, DeMoll C, Anderson KL, Griggs RB, Taylor BK, Porter NM, Thibault O (2015) Short-lived diabetes in the young-adult ZDF rat does not exacerbate neuronal Ca<sup>2+</sup> biomarkers of aging. *Brain Res* 1621:214–221. <https://doi.org/10.1016/j.brainres.2014.10.052>
  30. Salameh TS, Bullock KM, Hujuel IA, Niehoff ML, Wolden-Hanson T, Kim J, Morley JE, Farr SA, Banks WA (2015) Central nervous system delivery of intranasal insulin: mechanisms of uptake and effects on cognition. *J Alzheimers Dis* 47(3):715–728. <https://doi.org/10.3233/JAD-150307>
  31. Brini M, Carafoli E (2009) Calcium pumps in health and disease. *Physiol Rev* 89(4):1341–1378. <https://doi.org/10.1152/physrev.00032.2008>
  32. Clapham DE (2007) Calcium signaling. *Cell* 131(6):1047–1058. <https://doi.org/10.1016/j.cell.2007.11.028>
  33. Frazier HN, Maimaiti S, Anderson KL, Brewer LD, Gant JC, Porter NM, Thibault O (2017) Calcium's role as nuanced modulator of cellular physiology in the brain. *Biochem Biophys Res Commun* 483(4):981–987. <https://doi.org/10.1016/j.bbrc.2016.08.105>
  34. Jiang L, Bechtel MD, Galeva NA, Williams TD, Michaelis EK, Michaelis ML (2012) Decreases in plasma membrane Ca<sup>2+</sup>-ATPase in brain synaptic membrane rafts from aged

- rats. *J Neurochem* 123(5):689–699. <https://doi.org/10.1111/j.1471-4159.2012.07918.x>
35. Michaelis EK, Michaelis ML, Chang HH, Kito TE (1983) High affinity  $\text{Ca}^{2+}$ -stimulated  $\text{Mg}^{2+}$ -dependent ATPase in rat brain synaptosomes, synaptic membranes, and microsomes. *J Biol Chem* 258(10):6101–6108
  36. Michaelis ML, Michaelis EK (1981)  $\text{Ca}^{++}$  fluxes in resealed synaptic plasma membrane vesicles. *Life Sci* 28(1):37–45
  37. Schmidt N, Kollewe A, Constantin CE, Henrich S, Ritzau-Jost A, Bildl W, Saalbach A, Hallermann S, Kulik A, Fakler B, Schulte U (2017) Neuroplastin and basigin are essential auxiliary subunits of plasma membrane  $\text{Ca}^{2+}$ -ATPases and key regulators of  $\text{Ca}^{2+}$  clearance. *Neuron* 96(4):827–838 e829. <https://doi.org/10.1016/j.neuron.2017.09.038>
  38. Wang X, Michaelis EK (2010) Selective neuronal vulnerability to oxidative stress in the brain. *Front Aging Neurosci* 2:12. <https://doi.org/10.3389/fnagi.2010.00012>
  39. Khachaturian ZS (1989) The role of calcium regulation in brain aging: reexamination of a hypothesis. *Aging (Milano)* 1(1):17–34
  40. Landfield PW (1987) 'Increased calcium-current' hypothesis of brain aging. *Neurobiol Aging* 8(4):346–347
  41. Gant JC, Sama MM, Landfield PW, Thibault O (2006) Early and simultaneous emergence of multiple hippocampal biomarkers of aging is mediated by  $\text{Ca}^{2+}$ -induced  $\text{Ca}^{2+}$  release. *J Neurosci* 26(13):3482–3490. <https://doi.org/10.1523/JNEUROSCI.4171-05.2006>
  42. Kumar A, Foster TC (2005) Intracellular calcium stores contribute to increased susceptibility to LTD induction during aging. *Brain Res* 1031(1):125–128. <https://doi.org/10.1016/j.brainres.2004.10.023>
  43. Murchison D, McDermott AN, Lasarge CL, Peebles KA, Bizon JL, Griffith WH (2009) Enhanced calcium buffering in F344 rat cholinergic basal forebrain neurons is associated with age-related cognitive impairment. *J Neurophysiol* 102(4):2194–2207. <https://doi.org/10.1152/jn.00301.2009>
  44. Thibault O, Hadley R, Landfield PW (2001) Elevated postsynaptic  $[\text{Ca}^{2+}]_i$  and L-type calcium channel activity in aged hippocampal neurons: relationship to impaired synaptic plasticity. *J Neurosci* 21(24):9744–9756
  45. Thibault O, Landfield PW (1996) Increase in single L-type calcium channels in hippocampal neurons during aging. *Science* 272(5264):1017–1020
  46. Pancani T, Anderson KL, Brewer LD, Kadish I, DeMoll C, Landfield PW, Blalock EM, Porter NM, Thibault O (2013) Effect of high-fat diet on metabolic indices, cognition, and neuronal physiology in aging F344 rats. *Neurobiol Aging* 34(8):1977–1987. <https://doi.org/10.1016/j.neurobiolaging.2013.02.019>
  47. Maimaiti S, Anderson KL, DeMoll C, Brewer LD, Rauh BA, Gant JC, Blalock EM, Porter NM, Thibault O (2016) Intranasal insulin improves age-related cognitive deficits and reverses electrophysiological correlates of brain aging. *J Gerontol A* 71(1):30–39. <https://doi.org/10.1093/gerona/glu314>
  48. Wilkins HM, Harris JL, Carl SM, Lu EL, Eva Selfridge J, Roy J, Hutfles N, Koppel L, Morris S, Burns J, Michaelis JM, Michaelis ML, Brooks EK, Swerdlow WM RH (2014) Oxaloacetate activates brain mitochondrial biogenesis, enhances the insulin pathway, reduces inflammation and stimulates neurogenesis. *Hum Mol Genet* 23(24):6528–6541. <https://doi.org/10.1093/hmg/ddu371>
  49. Leibold DE, Nunez I, Chan M, Rosen OM (1991) Expression of inducible membrane-anchored insulin receptor kinase enhances deoxyglucose uptake. *J Biol Chem* 266(1):386–390
  50. Pancani T, Anderson KL, Porter NM, Thibault O (2011) Imaging of a glucose analog, calcium and NADH in neurons and astrocytes: dynamic responses to depolarization and sensitivity to pioglitazone. *Cell Calcium* 50(6):548–558. <https://doi.org/10.1016/j.ceca.2011.09.002>
  51. Pancani T, Phelps JT, Searcy JL, Kilgore MW, Chen KC, Porter NM, Thibault O (2009) Distinct modulation of voltage-gated and ligand-gated  $\text{Ca}^{2+}$  currents by PPAR-gamma agonists in cultured hippocampal neurons. *J Neurochem* 109(6):1800–1811. <https://doi.org/10.1111/j.1471-4159.2009.06107.x>
  52. Porter NM, Thibault O, Thibault V, Chen KC, Landfield PW (1997) Calcium channel density and hippocampal cell death with age in long-term culture. *J Neurosci* 17(14):5629–5639
  53. Furler S, Paterna JC, Weibel M, Bueler H (2001) Recombinant AAV vectors containing the foot and mouth disease virus 2A sequence confer efficient bicistronic gene expression in cultured cells and rat substantia nigra neurons. *Gene Ther* 8(11):864–873. <https://doi.org/10.1038/sj.gt.3301469>
  54. Mizuguchi H, Xu Z, Ishii-Watabe A, Uchida E, Hayakawa T (2000) IRES-dependent second gene expression is significantly lower than cap-dependent first gene expression in a bicistronic vector. *Mol Ther* 1(4):376–382. <https://doi.org/10.1006/mthe.2000.0050>
  55. Bodhinathan K, Kumar A, Foster TC (2010) Redox sensitive calcium stores underlie enhanced afterhyperpolarization of aged neurons: role for ryanodine receptor mediated calcium signaling. *J Neurophysiol* 104(5):2586–2593. <https://doi.org/10.1152/jn.00577.2010>
  56. Disterhoft JF, Thompson LT, Moyer JR Jr, Mogul DJ (1996) Calcium-dependent afterhyperpolarization and learning in young and aging hippocampus. *Life Sci* 59(5–6):413–420
  57. Kumar A, Foster TC (2004) Enhanced long-term potentiation during aging is masked by processes involving intracellular calcium stores. *J Neurophysiol* 91(6):2437–2444. <https://doi.org/10.1152/jn.01148.2003>
  58. Norris CM, Halpain S, Foster TC (1998) Reversal of age-related alterations in synaptic plasticity by blockade of L-type  $\text{Ca}^{2+}$  channels. *J Neurosci* 18(9):3171–3179
  59. Thibault O, Porter NM, Landfield PW (1993) Low  $\text{Ba}^{2+}$  and  $\text{Ca}^{2+}$  induce a sustained high probability of repolarization openings of L-type  $\text{Ca}^{2+}$  channels in hippocampal neurons: physiological implications. *Proc Natl Acad Sci USA* 90(24):11792–11796
  60. Landfield PW, Pitler TA (1984) Prolonged  $\text{Ca}^{2+}$ -dependent afterhyperpolarizations in hippocampal neurons of aged rats. *Science* 226(4678):1089–1092
  61. Wu WW, Oh MM, Disterhoft JF (2002) Age-related biophysical alterations of hippocampal pyramidal neurons: implications for learning and memory. *Ageing Res Rev* 1(2):181–207
  62. Berhanu P, Kolterman OG, Baron A, Tsai P, Olefsky JM, Brandenburg D (1983) Insulin receptors in isolated human adipocytes. Characterization by photoaffinity labeling and evidence for internalization and cellular processing. *J Clin Invest* 72(6):1958–1970. <https://doi.org/10.1172/JCI111160>
  63. Sonne O, Simpson IA (1984) Internalization of insulin and its receptor in the isolated rat adipose cell. Time-course and insulin concentration dependency. *Biochim Biophys Acta* 804(4):404–413
  64. Standaert ML, Pollet RJ (1984) Equilibrium model for insulin-induced receptor down-regulation. Regulation of insulin receptors in differentiated BC3H-1 myocytes. *J Biol Chem* 259(4):2346–2354
  65. Wang CC, Sonne O, Hedo JA, Cushman SW, Simpson IA (1983) Insulin-induced internalization of the insulin receptor in the isolated rat adipose cell. Detection of the internalized 138-kilodalton receptor subunit using a photoaffinity 125I-insulin. *J Biol Chem* 258(8):5129–5134
  66. Boyd FT Jr, Raizada MK (1983) Effects of insulin and tunicamycin on neuronal insulin receptors in culture. *Am J Physiol* 245(3):C283–287

67. Lee CC, Huang CC, Wu MY, Hsu KS (2005) Insulin stimulates postsynaptic density-95 protein translation via the phosphoinositide 3-kinase-Akt-mammalian target of rapamycin signaling pathway. *J Biol Chem* 280(18):18543–18550. <https://doi.org/10.1074/jbc.M414112200>
68. Kim EY, Dryer SE (2011) Effects of insulin and high glucose on mobilization of slo1 BKCa channels in podocytes. *J Cell Physiol* 226(9):2307–2315. <https://doi.org/10.1002/jcp.22567>
69. Benomar Y, Naour N, Aubourg A, Bailleux V, Gertler A, Djiane J, Guerre-Millo M, Taouis M (2006) Insulin and leptin induce Glut4 plasma membrane translocation and glucose uptake in a human neuronal cell line by a phosphatidylinositol 3-kinase-dependent mechanism. *Endocrinology* 147(5):2550–2556. <https://doi.org/10.1210/en.2005-1464>
70. Biessels GJ, Reagan LP (2015) Hippocampal insulin resistance and cognitive dysfunction. *Nat Rev Neurosci* 16(11):660–671. <https://doi.org/10.1038/nrn4019>
71. Grillo CA, Piroli GG, Lawrence RC, Wrighten SA, Green AJ, Wilson SP, Sakai RR, Kelly SJ, Wilson MA, Mott DD, Reagan LP (2015) Hippocampal insulin resistance impairs spatial learning and synaptic plasticity. *Diabetes* 64(11):3927–3936. <https://doi.org/10.2337/db15-0596>
72. McNay EC, Ong CT, McCrimmon RJ, Cresswell J, Bogan JS, Sherwin RS (2010) Hippocampal memory processes are modulated by insulin and high-fat-induced insulin resistance. *Neurobiol Learn Mem* 93(4):546–553. <https://doi.org/10.1016/j.nlm.2010.02.002>
73. Schubert M, Gautam D, Surjo D, Ueki K, Baudler S, Schubert D, Kondo T, Alber J, Galldiks N, Kustermann E, Arndt S, Jacobs AH, Krone W, Kahn CR, Bruning JC (2004) Role for neuronal insulin resistance in neurodegenerative diseases. *Proc Natl Acad Sci USA* 101(9):3100–3105. <https://doi.org/10.1073/pnas.0308724101>
74. Werner ED, Lee J, Hansen L, Yuan M, Shoelson SE (2004) Insulin resistance due to phosphorylation of insulin receptor substrate-1 at serine 302. *J Biol Chem* 279(34):35298–35305. <https://doi.org/10.1074/jbc.M405203200>
75. Blalock EM, Phelps JT, Pancani T, Searcy JL, Anderson KL, Gant JC, Popovic J, Avdiushko MG, Cohen DA, Chen KC, Porter NM, Thibault O (2010) Effects of long-term pioglitazone treatment on peripheral and central markers of aging. *PLoS ONE* 5(4):e10405. <https://doi.org/10.1371/journal.pone.0010405>
76. Sartorius T, Peter A, Heni M, Maetzler W, Fritsche A, Haring HU, Hennige AM (2015) The brain response to peripheral insulin declines with age: a contribution of the blood-brain barrier? *PLoS ONE* 10(5):e0126804. <https://doi.org/10.1371/journal.pone.0126804>
77. Stanley M, Macauley SL, Caesar EE, Koscal LJ, Moritz W, Robinson GO, Roh J, Keyser J, Jiang H, Holtzman DM (2016) The effects of peripheral and central high insulin on brain insulin signaling and amyloid-beta in young and old APP/PS1 mice. *J Neurosci* 36(46):11704–11715. <https://doi.org/10.1523/JNEUROSCI.2119-16.2016>
78. Abbott MA, Wells DG, Fallon JR (1999) The insulin receptor tyrosine kinase substrate p58/53 and the insulin receptor are components of CNS synapses. *J Neurosci* 19(17):7300–7308
79. Chiu SL, Chen CM, Cline HT (2008) Insulin receptor signaling regulates synapse number, dendritic plasticity, and circuit function in vivo. *Neuron* 58(5):708–719. <https://doi.org/10.1016/j.neuron.2008.04.014>
80. Zhao WQ, Alkon DL (2001) Role of insulin and insulin receptor in learning and memory. *Mol Cell Endocrinol* 177(1–2):125–134
81. Michaelis ML, Jiang L, Michaelis EK (2017) Isolation of synaptosomes, synaptic plasma membranes, and synaptic junctional complexes. *Methods Mol Biol* 1538:107–119. [https://doi.org/10.1007/978-1-4939-6688-2\\_9](https://doi.org/10.1007/978-1-4939-6688-2_9)